Heteroatom Chemistry
Volume 17, Number 3, 2006

[1-Me-1-*closo*-$SnB_{11}H_{11}$]$^-$ as a Potential Weakly Coordinating Anion: Synthesis of $Rh(PPh_3)_2$(1-Me-*closo*-$SnB_{11}H_{11}$) and Comparisons with $Rh(PR_3)_2$ (1-H-*closo*-$CB_{11}H_{11}$)

Eduardo Molinos, Thomas P. H. Player, Gabriele Kociok-Köhn, Giuseppe D. Ruggerio, and Andrew S. Weller

Department of Chemistry, University of Bath, Bath BA2 7AY, UK

Received 18 April 2005; revised 10 August 2005

ABSTRACT: *The closo-stannaborane salt [Rh(PPh$_3$)$_2$(nbd)][1-Me-1-closo-SnB$_{11}$H$_{11}$] reacts with H_2 in CH_2Cl_2 solution to afford the contact ion-pair Rh(PPh$_3$)$_2$(1-Me-closo-SnB$_{11}$H$_{11}$), which has been characterized in solution and the solid state by X-ray diffraction.* © 2006 Wiley Periodicals, Inc. Heteroatom Chem 17:174–180, 2006; Published online in Wiley InterScience (www.interscience.wiley.com). DOI 10.1002/hc.20218

INTRODUCTION

"Weakly coordinating" carborane monoanions based upon derivatives of [*closo*-$CB_{11}H_{12}$]$^-$ **I** find application in catalysis mediated by transition metal cations [1], the isolation of superacids [2], and the generation of coordinatively unsaturated complexes [3] that can have interesting structural features such as [M]$\cdots$$H_3C$ intermolecular interactions [4,5]. Given this, these anions are not as widely used as the fluorinated aryl borates, such as [$B(C_6H_3(CF_3)_2)_4$]$^-$ [6], even though they exhibit attractive properties such as being more chemically robust [2]. This, in part, may be due to the perception that the precursor to these carborane anions, [*closo*-$CB_{11}H_{12}$]$^-$, is not straightforward to prepare, needing multistep routes from non-routine starting materials that are relatively expensive and toxic, i.e., decaborane $B_{10}H_{14}$. Attractive routes to alleviate this problem by reducing the number of synthetic steps from *nido*-$B_{10}H_{14}$ [7,8], synthetic routes that start with Na[BH_4] to form *nido*-[$B_{11}H_{14}$]$^-$ and subsequent insertion of a {CR} vertex [9,10], or derivatization of [*closo*-$B_{12}H_{12}$]$^{2-}$ [11] have recently been reported. We report here an alternative approach to form precursors to weakly coordinating *closo*-icosahedral monoanionic borane species by use of the stanna borane [1-Me-*closo*-$SnB_{11}H_{11}$]$^-$, **II**. This cage species was first reported by Todd in 1992 by methylation of the dianion [*closo*-$SnB_{11}H_{11}$]$^{2-}$ [12]. This dianion, in turn, is available in two steps from Na[BH_4] in good yield and reasonable preparative scale (62%, $\sim$5 g). The coordination chemistry of [$SnB_{11}H_{11}$]$^{2-}$ has recently been elegantly explored by Wesemann [13–16] and this has centered around the interaction of the *exo*-lone pair on the cluster tin atom with metal centers. However, there are no reports of the use of monoanionic

Correspondence to: Andrew S. Weller; e-mail: a.s.weller@bath.ac.uk.
Contract grant sponsor: The Royal Society and the EPSRC.
Contract grant number: GR/S4270/01.

[1-R-*closo*-$SnB_{11}H_{11}]^-$ as potential weakly coordinating anion with transition metal fragments, although the potential to use such anions has been recognized [16] and as such they have been recently used to prepare ionic-liquids when partnered with imidazolium cations [17]. This short article reports a preliminary exploration of the transition metal chemistry of [1-R-*closo*-$SnB_{11}H_{11}]^-$ in the synthesis of the well-separated ion pair $[Rh(PPh_3)_2(nbd)][1\text{-}Me\text{-}closo\text{-}SnB_{11}H_{11}]$ and its subsequent treatment with dihydrogen to afford $Rh(PPh_3)_2$(1-Me-*closo*-$SnB_{11}H_{11}$). The $\{Rh(PPh_3)_2\}^+$ metal fragment has been chosen to partner the cage as we have previously reported on the synthesis and structures of this cation with anion **I**, and thus serves as a useful comparison to compare with stannaborane **II** [18].

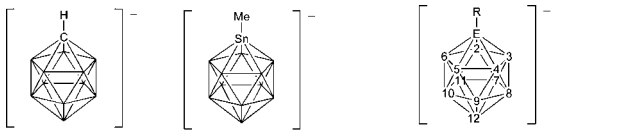

I **II** Numbering scheme for the [1-R-*closo*-$EB_{11}H_{11}$] anions

RESULTS

$[Rh(PPh_3)_2(nbd)][1\text{-}Me\text{-}closo\text{-}SnB_{11}H_{11}]$ **1** is prepared by reaction of $[Rh(nbd)Cl]_2$ (nbd = norbornadiene), $[Bu_4N][1\text{-}CH_3\text{-}closo\text{-}SnB_{11}H_{11}]$, and PPh_3 in methanol, and has been characterized by multinuclear NMR spectroscopy and microanalysis. In particular, the $^1H\{^{11}B\}$ spectrum shows three BH signals that also show coupling to $^{117/119}Sn$ at δ 2.97 (1H, J(SnH) 87), δ 2.06 (5H, J(SnH) 58), and δ 1.56 (5H, J(SnH) 35). The ^{11}B NMR spectrum ($CDCl_3$) shows two environments, at δ −10.4 (1 B) and δ −15.7 (10 B), and ^{11}B–Sn coupling is not resolved, even in the $^{11}B\{^1H\}$ NMR spectrum. In d_6-acetone, these signals resolve into three signals in the ratio 1:5:5. As it is well established that chemical shifts and J(BH) coupling constants can provide useful spectroscopic guides to the coordination of a cationic metal fragment with [*closo*-$CB_{11}H_{12}]^-$ [19], we have performed ^{11}B–^{11}B and ^{11}B–^1H correlation experiments on **1** to establish the identity of the signals. Todd has previously reported the ^{11}B–^{11}B COSY NMR data for the anion [1-Me-*closo*-$SnB_{11}H_{11}$][PPh_3CH_3] [12] and our results concur with these (see Experimental). In addition, a ^1H–^{11}B HMQC experiment allows the assignment of the ^1H signals to specific cluster vertices. These follow the pattern (low field to high field): BH(12), BH(7–11), and BH(2–6). The magnitude of ^1H–Sn coupling follows the reverse order, with BH(12) displaying the largest couple (J(SnH) 87) and BH(2–6) the smallest (J(SnH) 35): a demonstration of the antipodal effect in the NMR spectra of boranes [20]. The $^{31}P\{^1H\}$ NMR spectrum shows a single environment, δ 30.6 (J(RhP) 153).

Treatment of **1** with H_2 in CH_2Cl_2 solution results in a color change from orange to red/orange. $^1H\{^{11}B\}$ and $^{11}B\{^1H\}$ NMR spectroscopy indicate the formation of $Rh(PPh_3)_2$(1-Me-*closo*-$SnB_{11}H_{11}$) **2** (Scheme 1), the structure of which was confirmed in the solid state by an X-ray diffraction study (Fig. 1).

Compound **2** crystallizes with no close intermolecular contacts in the solid state. The refinement shows that the molecule crystallizes with a minor disordered component (10%). For the major (90%) component, the $\{Rh(PPh_3)_2\}^+$ fragment is coordinated through one upper pentagonal belt BH vertex (B2) and one lower pentagonal belt BH vertex (B11) through three center-two electron Rh–H–B interactions. The bond lengths around rhodium (see Table 1) are very similar to those observed in $Rh(PPh_3)_2$(1-H-*closo*-$CB_{11}H_{11}$) [18], Rh(cod)(1-H-*closo*-$CB_{11}H_{11}$) [21], and [$(Rh(PPh_3)_2\{7\text{-}Me\text{-}8\text{-}Ph\text{-}nido\text{-}C_2B_9H_{10})$] [22]. The Rh(I) fragment in **2** is square planar (sum of angles 360.0°). In the cluster, the Sn—B distances span the range 2.263(5)–2.323(4) Å which are similar to those observed in the parent [1-Me-*closo*-$SnB_{11}H_{11}]^-$ [12] anion, while there are no close contacts between the phenyl groups and the cage methyl group. The minor component in the

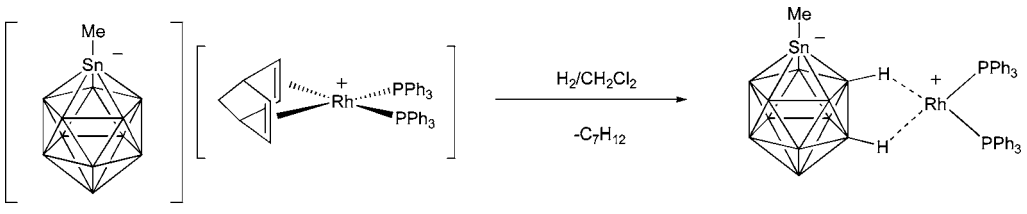

(1) **(2)**

SCHEME 1

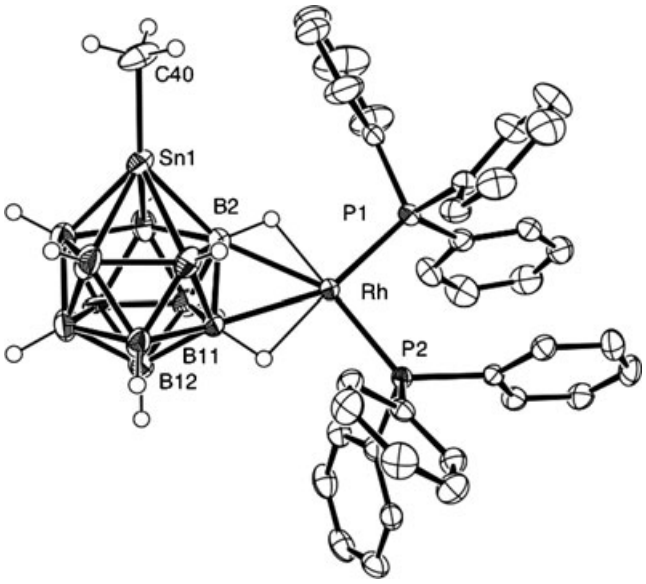

FIGURE 1 Solid-state structure of $Rh(PPh_3)_2$(1-Me-*closo*-$SnB_{11}H_{11}$) **2**. Thermal ellipsoids are shown at the 50% probability level, and hydrogen atoms associated with the phenyl groups are omitted for clarity. The major (90%) disordered component is shown.

crystal resolves best as the 7,8-isomer in which the $\{Rh(PPh_3)_2\}^+$ fragment coordinates to two BH vertices on the lower pentagonal belt. A B–H–[M] interaction between an upper belt BH vertex and an Au(I) center has been noted previously in $[Bu_3MeN][Au(1\text{-}Ph_2PCH_2\text{-}closo\text{-}SnB_{11}H_{11})_2]$ [16].

In solution, NMR spectroscopic data show that the $\{Rh(PPh_3)_2\}^+$ fragment is fluxional over the surface of the cage, affording C_5 symmetry for the anion, in contrast to the C_1 symmetry observed in the solid state. This fluxional process is not frozen out at -70°C in CD_2Cl_2 solution. The ^{1}H NMR spectrum shows signals due to PPh_3 and Sn–CH_3 in the ratio 30:3. The $^1H\{^{11}B\}$ NMR spectrum reveals three signals assigned to BH that also show coupling to Sn: δ 2.00 (1H, J(SnH) 80), δ 0.53 (5H, J(SnH) 50), and δ 0.05 (5H, J(SnH) ~40). As ^{11}B–^1H HMQC NMR experiments are not suitable for the assignments of these signals due to overlapping peaks in the ^{11}B NMR spectrum (vide infra), the magnitude of the J(SnH) coupling constant has been used to assign the BH signals, using the peak assignments made for **1** as a guide. These follow the order (high field to low field): BH(12), BH(7–11), and BH(2–6). Although this order follows that found in **1**, all the signals are shifted by approximately 1–2 ppm to higher field in **2**. Specifically, BH(12) is shifted by $\Delta\delta$ −0.97, BH(7–11) $\Delta\delta$ −1.53, and BH(2–6) $\Delta\delta$ −1.51. It is well established that the coordination of a metal fragment *exo* to the cage results in upfield chemical shift changes for those BH vertices interacting with the metal [18,23,24]. That BH(2–6) and BH(7–11) are shifted more than BH(12) suggests that, in solution, the $\{Rh(PPh_3)_2\}^+$ fragment interacts on the NMR timescale more with the BH(2–11) vertices and less with BH(12), consistent with the observed solid state structure that shows 2,11-coordination. The ^{11}B NMR spectrum shows two signals at δ −14.0 and δ −17.8, in the ratio 1:10—the latter being a 5 + 5 coincidence. These signals have also been shifted upfield from **1**, by ca. $\Delta\delta$ −4 ppm, again suggesting that the $\{Rh(PPh_3)_2\}^+$ fragment interacts with the entire BH surface of the cage anion.

DISCUSSION

Reduction of the norbornadiene ligand in **1** with H_2 results in a coordinatively unsaturated $\{Rh(PPh_3)_2\}^+$ fragment that coordinates with the stannaborane [1-Me-*closo*-$SnB_{11}H_{11}$]$^-$ anion through two B—H—Rh three center-two electron bonds. Both the solid state and solution data for **2** can be contrasted with those for the carborane anion complexes $Rh(PR_3)_2$(1-H-*closo*-$CB_{11}H_{11}$) (R = Ph **III** [18], Cy **IV** [19]) (Scheme 2). Both **III** and **IV** show interactions with the lower hemisphere of the carborane cage. In solution, the $^1H\{^{11}B\}$ NMR spectra show this by large ($\Delta\delta$ca. −5 ppm) upfield shifts of BH(12), smaller shifts for B(7–11) of $\Delta\delta$a. −1 to −2 ppm and virtually no chemical shift change for B(2–6). Similar chemical shift changes are also observed

TABLE 1 Selected Bond Lengths (Å) and Angles (°) for **2**

Bond length (Å)					
Rh—P1	2.2155(8)	Rh—P2	2.2417(8)	Rh—B2	2.369(4)
Rh—B11	2.372(4)	Sn—B2	2.273(4)	Sn—B3	2.292(4)
Sn—B4	2.263(5)	Sn—B5	2.322(5)	Sn—B6	2.323(4)
Rh—H2	1.85(4)	Rh—H11	1.89(3)		
Bond angle (°)					
P1—Rh—P2	95.64(3)	P1—Rh—B2	111.53(10)	B2—Rh—B11	42.71(13)
B11—Rh—P2	110.15(9)	C40—Sn1—B12	173.1(1)		

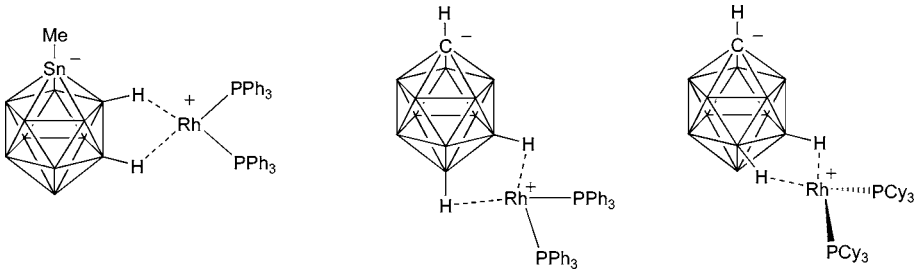

(2) III IV

SCHEME 2

in the $^{11}B\{^1H\}$ NMR spectrum. In the solid state, **III** coordinates through BH(12)/BH(7) while **IV** coordinates through BH(7)/BH(8), both being consistent with NMR data and with the model complex $Rh(PMe_3)_2$(1-H-*closo*-$CB_{11}H_{11}$) in which there is essentially no difference energetically between these two isomers [19]. In contrast, stannaborane **2** coordinates in the solid state through one upper pentagonal belt BH vertex and one lower pentagonal belt vertex. However, in solution, the metal fragment must be fluxional over the *whole* BH surface as all the BH signals show upfield shifts on coordination of the $\{Rh(PPh_3)_2\}^+$ fragment. That BH(2–6) and BH(7–11) show larger chemical shifts ($\Delta\delta$ca. −1.5) than BH(12) ($\Delta\delta$ca. −1) suggests that the metal fragment spends relatively less time coordinated with BH(12) on the NMR timescale.

The different coordination modes of the $\{Rh(PPh_3)_2\}^+$ fragment between the stannaborane and carborane cages can be explained at a basic level—ignoring the orbital contributions to the bonding—by using a simple analysis of the charge distribution in the two cages. For [1-H-*closo*-$CB_{11}H_{11}]^-$, the relative electronegativity of carbon and boron means that upper belt vertices, BH(2–6), would be expected to be relatively positively charged, while the lower hemisphere of the cage would be relatively negatively charged. Previous calculations at the DFT level have confirmed this [4,25]. For comparison with [1-Me-*closo*-$SnB_{11}H_{11}]^-$, we have performed calculations at the B3LYP/DZVP level on [1-Me-*closo*-$CB_{11}H_{11}]^-$ and this shows a very similar charge distribution (based on NBO analysis) as reported previously for [1-H-*closo*-$CB_{11}H_{11}]^-$ [4,25] (Fig. 2). For the stannaborane [1-Me-*closo*-$SnB_{11}H_{11}]^-$, this polarization would be expected to be reversed, as the tin is electropositive compared with boron, and DFT calculations show all the BH vertices as having a negative charge, with BH(2–6) being more negative, followed by BH(7–11) and BH(12) (Fig. 2). On purely electrostatic grounds, coordination of a metal fragment with [*closo*-$CB_{11}H_{12}]^-$ would be expected to occur with the lower hemisphere of the cage—as is observed both in the solid state (e.g., **III** and **IV**) and in solution. With [1-Me-*closo*-$SnB_{11}H_{11}]^-$, having all BH vertices negatively charged, a metal fragment would be expected to coordinate with the entire BH surface of the cage. That, for **2**, all the BH signals shift to high-field in the $^1H\{^1B\}$ and ^{11}B NMR spectra, with B(2–11) shifting the most, and the X-ray structure shows coordination of the metal fragment to BH(2) and BH(11), is consistent with this analysis.

CONCLUSIONS

The synthesis of [1-Me-1-*closo*-$SnB_{11}H_{11}$][NBu_4] in multigram quantities from Na[BH_4] suggests that it might be a more accessible alternative to [*closo*-$CB_{11}H_{12}]^-$, the derivatives of which have been shown to be some of the most robust weakly coordinating anions currently known. Although this cage is relatively tightly bound to metal fragment in **2**, it is well documented that introducing between 6 and 11 halogen or methyl groups to the periphery of [*closo*-$CB_{11}H_{12}]^-$ make the resulting anion significantly more weakly coordinating. It will be interesting to see if analogous derivatives of [1-Me-1-*closo*-$SnB_{11}H_{11}]^-$ can be prepared and if these show the same attractive properties as their carborane analogous.

EXPERIMENTAL

General

All manipulations were carried out under an atmosphere of argon, using standard Schlenk-line and glove-box techniques. Glassware were pre-dried in an oven at 130°C and flamed with a blowtorch under vacuum prior to use. Solvents were purified using an MBaun SPS column system. CD_2Cl_2 was dried over

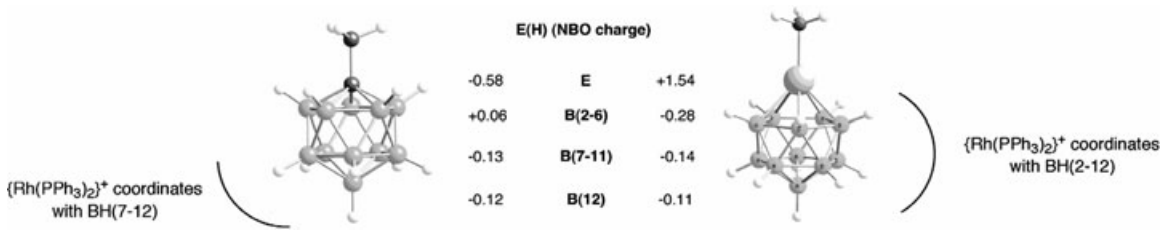

FIGURE 2 Charges on each unique {BH} and {E} vertex as calculated by the NBO analysis at the B3LYP/DZVP level.

CaH_2 and distilled under vacuum. $[Rh(nbd)Cl]_2$ [26] was prepared as described previously. $[Bu_4N][1\text{-}CH_3\text{-}closo\text{-}SnB_{11}H_{11}]$ was prepared by addition of MeI to $[NBu_4]_2[closo\text{-}SnB_{11}H_{11}]$ as described by Todd for the $[MePPh_3]$ salt [12]. The $[NBu_4]_2[closo\text{-}SnB_{11}H_{11}]$ is prepared exactly as outlined by Todd [12] for $[MePPh_3]_2[closo\text{-}SnB_{11}H_{11}]$ from $[Me_3NH][B_{11}H_{14}]$ substituting $[NBu_4]Cl$ for $[MePPh_3]Cl$ in the final step. Microanalyses were performed by Mr. Alan Carver (University of Bath microanalytical service).

NMR Spectroscopy

^1H, $^1H\{^{11}B\}$, ^{11}B, $^{11}B\{^1H\}$, and $^{31}P\{^1H\}$ NMR spectra were recorded on Bruker Avance 300 or 400 MHz spectrometers. Residual protio solvent was used as reference for ^1H. ^{11}B and ^{31}P were referenced to external $BF_3{\cdot}OEt_2$ and 85% H_3PO_4, respectively. Values are quoted in ppm. Coupling constants are given in Hz.

X-ray Crystallography

The crystal structure data for **2** were collected on a Nonius KappaCCD diffractometer with details provided in Table 2. Structure solution, followed by full-matrix least squares refinement was performed using the SHELXL suite of programs throughout [27]. Hydrogen atoms were included in calculated positions apart from those associated with the Rh—H—B bonds, which were located in the final difference map and refined without constraints. Crystallographic data files have been deposited with the Cambridge Crystallographic Data Centre (CCDC xxxxxx), 12 Union Road, Cambridge CB2 1EZ, UK; Tel.: (+44) 1223-336-408; Fax: (+44) 1223-336-033; e-mail: deposit@ccdc.cam.ac.uk.

$[Rh(PPh_3)_2(nbd)][1\text{-}Me\text{-}closo\text{-}SnB_{11}H_{12}]$ **1**. $[Rh(nbd)Cl]_2$ (39.2 mg, 0.085 mmol) was placed in a Schlenk tube and MeOH (5 cm^3) added via cannula to give a yellow suspension. After addition of triphenylphosphine (89.1 mg, 0.34 mmol), the reaction mixture was stirred until complete dissolution. Addition of $[Bu_4N][1\text{-}CH_3\text{-}closo\text{-}SnB_{11}H_{11}]$ (86.0 mg, 0.17 mmol) led to the formation of an orange precipitate, which was washed with cold MeOH (2×1 mL) and dried under vacuum. The product was recrystallized from CH_2Cl_2/pentane to afford 107 mg (0.108 mmol, yield = 64%).

NMR data (assignments from ^{11}B–^{11}B COSY and ^{11}B–^1H HMQC). δ $^1H\{^{11}B\}$ ($CDCl_3$, 298 K): 7.34 (m, 30H, Ph), 4.50 (s, 4H, nbd), 4.11 (s, 2H, nbd), 2.97 (s, 1H, BH(12), J(SnH) 87), 2.06 (s, 5H, BH(7–11), J(SnH) 58), 1.69 (s, 3H, Sn—CH_3, J(SnH) 88), 1.56 (s, 5H, BH(2–6), J(SnH) 35). $\delta^{11}B$ ($CDCl_3$, 298 K): −10.4 (d, 1B, B(12), J(HB) 133), −15.7 (d, 10B, B(2–11), J(HB) 153). $\delta^{11}B$ ($(CD_3)_2CO$, 298 K): −11.5 (d, 1B, B(12), J(HB) 134), −16.6 (d, 5B, B(7–11), J(HB) 116), −17.4 (d, 5B, B(2–6), J(HB) 122). $\delta^{31}P$ ($CDCl_3$, 298 K): 30.6 (d, 2P, J(RhP) 153). $C_{46}H_{58}B_{11}P_2RhSn$ requires: C, 54.52; H, 5.77%; Found: C 54.1, H 6.68%.

$Rh(PPh_3)_2(1\text{-}Me\text{-}closo\text{-}SnB_{11}H_{11})$ **2**. $[Rh(PPh_3)_2(nbd)][1\text{-}CH_3\text{-}closo\text{-}SnB_{11}H_{11}]$ (10 mg, 0.010 mmol) was placed in a 15 cm^3 Young's ampoule and CH_2Cl_2 (4 cm^3) was added via cannula. The solution was freeze–pump–thawed three times. After the third cycle, the solution was opened to a H_2 atmosphere (1 atm). The ampoule was closed and the solution stirred for 30 min. Then, the solvent was evaporated and the red residue dried in vacuo. Yield was quantitative by NMR spectroscopy. Crystals suitable for an X-ray diffraction study were grown from a CD_2Cl_2/pentane solution at room temperature.

NMR data. δ $^1H\{^{11}B\}$ (CD_2Cl_2, 298 K): 7.40 (m, 12H, Ph), 7.28 (m, 6H, Ph), 7.14 (m, 12H, Ph), 2.00 (s, 1H, BH(12), J(SnH) 80), 1.53 (s, 3H, Sn—CH_3, J(SnH) 92), 0.53 (s, 5H, B(7–11), J(SnH) 50), 0.05 (s, 5H, BH(2–6), J(SnH) ∼40). $\delta^{11}B$ (CD_2Cl_2, 298 K): −14.0 (d, 1B, B(12), J(HB) 129), −17.8 (d, 5 + 5 coincidence, J(HB) 120). $\delta^{31}P$ (CD_2Cl_2, 298 K): 45.7 (d, 2P, J(RhP) 188). $C_{37}H_{44}B_{11}P_2RhSn$ requires: C, 49.86; H, 4.98%; Found: C 50.5, H 4.94%.

DFT Calculations

The Gaussian 98 program was employed with the DZVP basis set for B3LYP gas-phase geometry

TABLE 2 Crystal Data and Structure Refinement for Compound **1**

Empirical formula	$C_{37}H_{44}B_{11}P_2RhSn$
Formula weight	891.17
Temperature (K)	150(2)
Wavelength (Å)	0.71073
Crystal system	Monoclinic
Space group	*C*2/*c*
a (Å)	32.1840(3)
b (Å)	32.1840(3)
c(Å)	18.9180(2)
α (°)	90
β(°p)	117.4640(10)
(γ°)	90
Volume ($Å^3$)	7971.77(16)
Z	8
Density (calculated) (mg/m^3)	1.485
Absorption coefficient (mm^{-1})	1.149
F(0 0 0)	3568
Crystal size (mm)	$0.40 \times 0.33 \times 0.33$
Theta range for data collection (°)	3.02–27.53
Reflections collected	68622
Independent reflections	9139 ($R_{int} = 0.0697$)
Absorption correction	Semi-empirical from equivalents
Data Completeness	99.4
Refinement method	Full-matrix least-squares on F^2
Data/restraints/parameters	9139/0/495
Goodness-of-fit on F^2	1.143
Final *R* indices ($I > 2\sigma(I)$)	$R_1 = 0.0481$, $wR_2 = 0.0803$
R indices (all data)	$R_1 = 0.0650$, $wR_2 = 0.0847$
Largest diff. peak and hole (e $Å^{-3}$)	0.999 and −0.879

optimizations, using the Berny routine algorithm [28]. No symmetry constraints were imposed, and the nature of each stationary point was verified through frequency calculations.

REFERENCES

[1] (a) Macchioni, A. Chem Rev 2005, 105, 2039; (b) Krossing, I.; Raabe, I. Angew Chem, Int Ed 2004, 43, 2066.
[2] Reed, C. A. Chem Commun 2005, 1669.
[3] Reed, C. A. Acc Chem Res 1998, 31, 133.
[4] Zharov, I.; Weng, T.-C.; Orendt, A. M.; Barich, D. H.; Penner-Hahn, J.; Grant, D. M.; Havlas, Z.; Michl, J. J Am Chem Soc 2004, 126, 12033.
[5] Ingleson, M. J.; Patmore, N. J.; Kociok-Köhn, G.; Mahon, M. F.; Ruggiero, G. D.; Weller, A. S.; Clarke, A. J.; Rourke, J. P. J Am Chem Soc 2004, 126, 1503.
[6] Chen, E. Y. X.; Marks, T. J Chem Rev 2000, 100, 1391.
[7] Batsanov, A. S.; Fox, M. A.; Goeta, A. E.; Howard, J. A. K.; Hughes, A. K.; Malget, J. M. J Chem Soc, Dalton Trans 2002, 2624.
[8] Brellochs, B.; Backovsky, J.; Stibr, B.; Jelinek, T.; Holub, J.; Bakardjiev, M.; Hnyk, D.; Hofmann, M.; Cisarova, I.; Wrackmeyer, B. Eur J Inorg Chem 2004, 3605.
[9] Franken, A.; King, B. T.; Rudolph, J.; Rao, P.; Noll, B. C.; Michl, J. Coll Czech Chem Commun 2001, 66, 1238.
[10] Korbe, S.; Sowers, D. B.; Franken, A.; Michl, J. Inorg Chem 2004, 43, 8158.
[11] Ivanov, S. V.; Davis, J. A.; Miller, S. M.; Anderson, O. P.; Strauss, S. H. Inorg Chem 2003, 42, 4489.
[12] Chapman, R. W.; Kester, J. G.; Folting, K.; Streib, W. E.; Todd, L. J. Inorg Chem 1992, 31, 979.
[13] Wesemann, L. Z. Anorg All Chem 2004, 630, 1349.
[14] Marx, T.; Mosel, B.; Pantenburg, I.; Hagen, S.; Schulze, H.; Wesemann, L. Chem Eur J 2003, 9, 4472.
[15] Hagen, S.; Pantenburg, I.; Weigend, F.; Wickleder, C.; Wesemann, L. Angew Chem 2003, 42, 1501.
[16] Ronig, B.; Schulze, H.; Pantenburg, I.; Wesemann, L. Eur J Inorg Chem 2005, 314.
[17] Ronig, B.; Pantenburg, I.; Wesemann, L. Eur J Inorg Chem 2002, 319.
[18] Rifat, A.; Patmore, N. J.; Mahon, M. F.; Weller, A. S. Organometallics 2002, 21, 2856–2865.
[19] Rifat, A.; Laing, G.; Kociok-Köhn, G.; Mahon, M. F.; Ruggiero, G. D.; Weller, A. S. J Organometal Chem 2003, 680, 127.
[20] Hermánek, S. Chem Rev 1992, 92, 325.
[21] Weller, A. S.; Mahon, M. F.; Steed, J. W. J Organomet Chem 2000, 614–615, 113–119.
[22] Knobler, C. B.; Marder, T. B.; Mizusawa, E. A.; Teller, R. G.; Long, J. A.; Behnken, P. E.; Hawthorne, M. F. J Am Chem Soc 1984, 106, 2990.
[23] Patmore, N. J.; Mahon, M. F.; Steed, J. W.; Weller, A. S. J Chem Soc, Dalton Trans 2001, 277.

[24] Crowther, D. J.; Borkowsky, S. L.; Swenson, D.; Meyer, T. Y.; Jordan, R. F. Organometallics 1993, 12, 2897–2903.
[25] McKee, M. L. J Am Chem Soc 1997, 119, 4220.
[26] Haines, L. M. Inorg Chem 1970, 9, 1517.
[27] Sheldrick, G. M. SHELX-97. University of Göttingen; A computer program for refinement of crystal structures; 1997.
[28] Frisch, M. J.; Trucks, G. W.; Schlegel, H. B.; Scuseria, G. E.; Robb, M. A.; Cheeseman, J. R.; Zakrzewski, V. G.; Montgomery, J. A.; Stratmann, R. E.; Burant, J. C.; Dapprich, S.; Millam, J. M.; Daniels, A. D.; Kudin, K. N.; Strain, M. C.; Farkas, O.; Tomasi, J.; Barone, V.; Cossi, M.; Cammi, R.; Mennucci, B.; Pomelli, C.; Adamo, C.; Cliord, S.; Ochterski, J.; Petersson, G. A.; Ayala, P. Y.; Cui, Q.; Morokuma, K.; Malick, D. K.; Rabuck, A. D.; Raghavachari, K.; Foresman, J. B.; Cioslowski, J.; Ortiz, J. V.; Stefanov, B. B.; Liu, G.; Liashenko, A.; Piskorz, P.; Komaromi, I.; Gomperts, R.; Martin, R. L.; Fox, D. J.; Keith, T.; Al-Laham, M. A.; Peng, C. Y.; Nanayakkara, A.; Gonzalez, C.; Challacombe, M.; Gill, P. M. W.; Johnson, B.; Chen, W.; Wong, M. W.; Andres, J. L.; Gonzalez, C.; Head-Gordon, M.; Replogle, E. S.; Pople, J. A.; Gaussian, Inc.: Pittsburgh, PA, 1998.